

# Comparison of Photocatalytic Performance of Different Types of Graphene in Fe<sub>3</sub>O<sub>4</sub>/SnO<sub>2</sub> Composites

Valentinus Paramarta<sup>1,2</sup>, Ardiansyah Taufik<sup>1,2</sup>, Rosari Saleh<sup>1,2,\*</sup>

<sup>1</sup>Departemen Fisika, Fakultas MIPA-Universitas Indonesia, 16424 Depok, Indonesia

<sup>2</sup>Integrated Laboratory of Energy and Environment, Fakultas MIPA-Universitas Indonesia, 16424 Depok, Indonesia

E-mail: rosari.saleh@gmail.com

**Abstract.** We have reported the role of annealing temperature Fe<sub>3</sub>O<sub>4</sub>/SnO<sub>2</sub> nanocomposites as a photocatalyst for remove methylene blue (MB) dye from aqueous solution. However, how to enhanced the degradation performance of Fe<sub>3</sub>O<sub>4</sub>/SnO<sub>2</sub> nanocomposites is important to its photocatalytic application. Therefore, in this work Fe<sub>3</sub>O<sub>4</sub>/SnO<sub>2</sub> nanocomposites was combined with two different types of graphene materials (NGP and grahene) to improve the photocatalytic performance for remove methylene blue (MB) dye. Fe<sub>3</sub>O<sub>4</sub>/SnO<sub>2</sub>/NGP and Fe<sub>3</sub>O<sub>4</sub>/SnO<sub>2</sub>/graphene have been successfully synthesized by co-precipitation method. The influence of two types graphene on Fe<sub>3</sub>O<sub>4</sub>/SnO<sub>2</sub> nanocomposites properties were systematically investigated by means of X-ray diffraction (XRD), Fourier transform infrared (FTIR) spectroscopy and Thermal gravimetric analysis (TGA). Degradation of methylene Blue (MB) in aqueous solution was studied in detail under photocatalytic process. Effect of catalyst dosage (0.1-0.4 g/L) and scavengers on dye degradation were carried out to check the efficiency of photocatalyst. The results indicated Fe<sub>3</sub>O<sub>4</sub>/SnO<sub>2</sub>/graphene displayed higher photocatalytic activity than other catalyst. The reusability tests have also been done to ensure the stability of the used photocatalyst.

## 1. Introduction

In recent years heterogeneous photocatalysis has attracted much attention to developed sustainable technologies for energy production and storage, green chemical synthesis, and water treatments [1-2]. Semiconductor nanoparticles are useful as an effective technique to eliminate pollutants from air and wastewater due to their unique optical and electronic properties [3]. Among various semiconductor nanoparticles, such as SiC, TiO<sub>2</sub>, ZnO, Fe<sub>2</sub>O<sub>3</sub>, WO<sub>3</sub>, SnO<sub>2</sub> nanoparticles have attracted considerable attention because of their high physicochemical stability, low cost, lack of toxicity, easy production, and good photoactivity [4-6]. Because of their several advantages, SnO<sub>2</sub> potentially to be ideal catalyst. However, as a photocatalyst, SnO<sub>2</sub> has several fundamental issue for photocatalytic application such as: (1) the difficulty process of splitting the catalyst material from dye waste after photocatalytic process [7]; (2) The recombination rate of electron and hole pairs are too rapid [8].

To overcome the problem, one strategy is to make magnetically separable photocatalyst for recovery and reuse of SnO<sub>2</sub> nanoparticle [9]. Combining SnO<sub>2</sub> nanoparticle with magnetic material such as Fe<sub>3</sub>O<sub>4</sub> was used to enhance separation properties of the photocatalyst from the treated water [10]. Furthermore, hybridizing SnO<sub>2</sub> nanoparticle with graphene materials is a good method to enhance the photocatalytic activity of SnO<sub>2</sub> for degrade organic dyes by enhancing the electron mobility and also inhibit the recombination of photogenerated electron and hole pairs. Due to



graphene properties such as excellent electronic conductivity, mechanical properties and high surface area [11]. Therefore, it is believed that, combining  $\text{SnO}_2$ ,  $\text{Fe}_3\text{O}_4$  and graphene materials would exhibit excellent photocatalytic performance with highly effectively recovery by magnetic separation technique.

In this study,  $\text{Fe}_3\text{O}_4/\text{SnO}_2$  nanoparticle will be combined with two different types of graphene materials: 1) nanographene platelets (NGP); 2) graphene that are applied as photocatalyst to degrade methylene blue (MB) dye. To hybridize with graphene materials,  $\text{Fe}_3\text{O}_4/\text{SnO}_2/\text{NGP}$  and  $\text{Fe}_3\text{O}_4/\text{SnO}_2/\text{graphene}$  nanocomposites were prepared using co-precipitation method. Photocatalyst powders are characterized by using X-ray diffraction (XRD), Fourier transform infrared (FTIR) spectroscopy and Thermal gravimetric analysis (TGA). In the present study, the photocatalytic activity of the  $\text{Fe}_3\text{O}_4/\text{SnO}_2$  nanocomposites with two different types of graphene materials were analyzed using methylene blue as organic pollutant model in aqueous solution under UV light irradiation. As expected, the result shows  $\text{Fe}_3\text{O}_4/\text{SnO}_2$  combined with graphene materials exhibit better photocatalytic performance than  $\text{Fe}_3\text{O}_4/\text{SnO}_2$  for degradation of methylene blue (MB).

## 2. Experimental

### 2.1. Chemicals

All reagents used were analytical grade and were used without further purification. Anhydrous tin chloride ( $\text{SnCl}_2$ ), iron (II) sulfate heptahydrate ( $\text{FeSO}_4 \cdot 7\text{H}_2\text{O}$ ), sodium hydroxide (NaOH), methylene blue (MB), ethanol, ethylene glycol (EG) were purchased from Merck (Kenilworth, NJ, USA). Graphene and nanographene platelets (NGP) were bought from Angstrom Material.

### 2.2. Preparation of $\text{SnO}_2$ nanoparticle and $\text{Fe}_3\text{O}_4/\text{SnO}_2$ nanocomposites

The  $\text{Fe}_3\text{O}_4$  nanoparticles were synthesized using the same method used in our previous study [12]. The  $\text{SnO}_2$  nanoparticles were synthesized using a modification of the method reported by Yue Li and co-workers [13]. First,  $\text{SnCl}_2$  was dissolved in a mixture of ethanol and aqueous solution, which was then added into the NaOH solutions using magnetic stirring. Then, the mixed solutions were heated at 180 °C for 3 h, then chilled to room temperature. The precipitate was obtained by centrifugation and washed using aqueous solutions and ethanol several times. The precipitated particles were dried under vacuum at 80 °C, and  $\text{SnO}_2$  particles were obtained by calcination for 3 h at 700 °C.

The  $\text{Fe}_3\text{O}_4/\text{SnO}_2$  nanocomposites were synthesized using the sol-gel method. First,  $\text{SnO}_2$  nanoparticles were mixed with  $\text{Fe}_3\text{O}_4$  in a mixture of ethanol and aqueous solution. Each mixture was ultrasonicated for 2 h and then centrifuged to obtain the precipitate. The resulting product was then dried under vacuum at 80 °C for 12 h to obtain  $\text{Fe}_3\text{O}_4/\text{SnO}_2$  nanocomposites with the molar ratio 1:2.

### 2.3. Preparation of $\text{Fe}_3\text{O}_4/\text{SnO}_2/\text{NGP}$ and $\text{Fe}_3\text{O}_4/\text{SnO}_2/\text{graphene}$ composites

$\text{Fe}_3\text{O}_4/\text{SnO}_2/\text{graphene}$  is synthesized using the hydrothermal method. First, graphene is dissolved into DI water and ethanol through ultrasonic treatment for 2 hours, then  $\text{Fe}_3\text{O}_4/\text{SnO}_2$  nanocomposites is poured into the solution and stirred magnetically. The mixed solution is then heated at 120 °C for 3 hours. The result of solution is then centrifuged and dried at 70 °C under vacuum condition. The same method is also applied to synthesize  $\text{Fe}_3\text{O}_4/\text{SnO}_2/\text{NGP}$ .

### 2.4. Characterization

The sample was characterized by XRD using a Rigaku Miniflex 600 (Rigaku, Tokyo, Japan) with a Cu K- $\alpha$  radiation source ( $\lambda = 1.5406 \text{ \AA}$ ), the spectrum of infrared absorption from the samples is obtained using Shimadzu FTIR spectrophotometer in the range of 400-4000  $\text{cm}^{-1}$  and thermal gravimetric analysis (TGA) of the sample is obtain using Rigaku TG8121 with the temperature from 27°C until 900°C.

### 2.5. Photocatalytic experiments

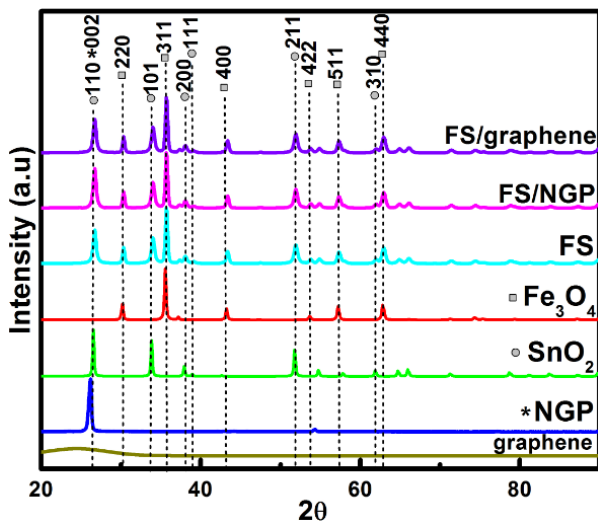


**FIGURE 1.** XRD pattern of Fe<sub>3</sub>O<sub>4</sub>/SnO<sub>2</sub> nanocomposite, Fe<sub>3</sub>O<sub>4</sub>/SnO<sub>2</sub>/NGP and Fe<sub>3</sub>O<sub>4</sub>/SnO<sub>2</sub>/graphene composites.

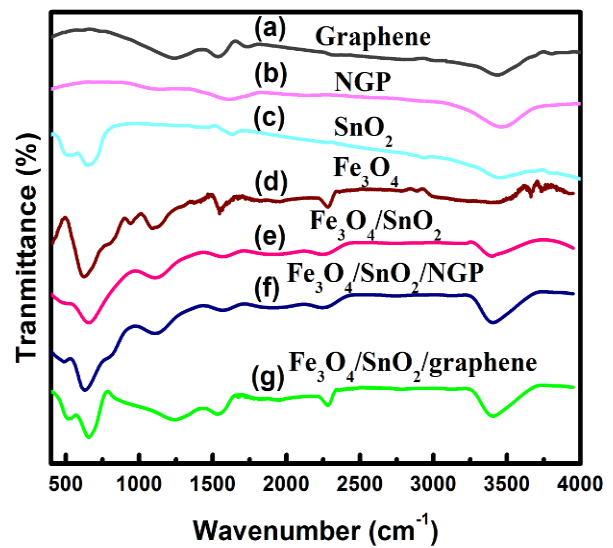


**FIGURE 2.** FTIR spectra of (e) Fe<sub>3</sub>O<sub>4</sub>/SnO<sub>2</sub> nanocomposite, (f) Fe<sub>3</sub>O<sub>4</sub>/SnO<sub>2</sub>/NGP and (g) Fe<sub>3</sub>O<sub>4</sub>/SnO<sub>2</sub>/graphene composites.

The photocatalytic experiment was done by mixing the sample into 100mL methylene blue (MB) solutions used as pollutant model with concentrations 20mg/L respectively, and pH solutions adjusted NaOH. The solution was allowed to stand in stirring state for adsorption and desorption balance. The photocatalytic test, the solution was given UV light irradiation with power 40W and wavelength of 320-400 nm. The solution was given UV light irradiation for 2 hours. Every 15 minutes span the concentration of MB solution was analyzed using UV-vis spectrometer. The maximum degradation were calculated using the following equation:

$$\text{Maximum degradation (\%)} = \frac{(C_0 - C_t)}{C_0} \times 100\% \quad (1)$$

where C<sub>0</sub> is the initial concentration of MB dye solution (mg/L), C<sub>t</sub> is the concentration of dye at certain irradiation time (mg/L).

### 2.6. Scavenger experiments

To determine the most influential species in sonocatalytic activity, it was given the difference radical-scavenger in methylene blue (MB) solution. Ammonium oxalate, sodium sulfate, and tert-butyl alcohol (TBA) were used each for scavenger hole, electron and hydroxyl radical. The measurement done in the same way as described above.

### 3. Result

The X-ray diffraction (XRD) patterns of the Fe<sub>3</sub>O<sub>4</sub>/SnO<sub>2</sub> nanocomposite, Fe<sub>3</sub>O<sub>4</sub>/SnO<sub>2</sub>/NGP and Fe<sub>3</sub>O<sub>4</sub>/SnO<sub>2</sub>/graphene composites which labeled as FS, FS/NGP and FS/graphene are shown in Fig. 1, respectively. The diffraction pattern of Fe<sub>3</sub>O<sub>4</sub> sample observed at the value 2θ = 30.14°, 35.49°, 43.28°, 57.20°, 62.83° and 74.8° which shows each area (220), (311), (400), (511), (440) and (533) of the cubic spinel structure. Diffraction pattern of SnO<sub>2</sub> nanoparticle sample observed at value 2θ = 26.5°, 33.8°, 38°, 39°, 51.8°, 54.8°, 58°, 62°, 64.7°, 65.8°, 71.2°, 78.2°, 81.2°, 83.7° which shows the existence of areas (110), (101), (200), (111), (211), (220), (002), (310), (112), (301), (202), (321), (400), (222) of tetragonal structure of SnO<sub>2</sub> nanoparticle. The XRD pattern of Fe<sub>3</sub>O<sub>4</sub>/SnO<sub>2</sub> nanocomposites shows the existence of cubic spinel phase of Fe<sub>3</sub>O<sub>4</sub>, followed by the addition of tetragonal SnO<sub>2</sub> nanocomposites. The peak at 2θ of 26.0° indicates (002) plane of the NGP structure. For graphene, there is only a broad peak at around 2θ of 25°, which indicates the structure of

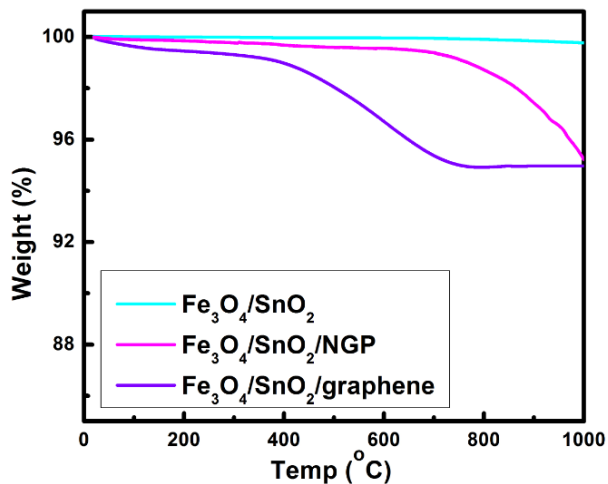


**FIGURE 3.** TGA curve of Fe<sub>3</sub>O<sub>4</sub>/SnO<sub>2</sub> nanocomposite, Fe<sub>3</sub>O<sub>4</sub>/SnO<sub>2</sub>/NGP and Fe<sub>3</sub>O<sub>4</sub>/SnO<sub>2</sub>/graphene composites.

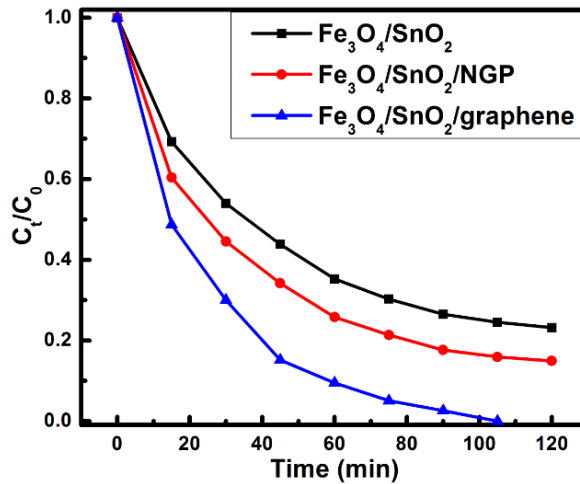


**FIGURE 4.** Photocatalytic degradation of Fe<sub>3</sub>O<sub>4</sub>/SnO<sub>2</sub> nanocomposite, Fe<sub>3</sub>O<sub>4</sub>/SnO<sub>2</sub>/NGP and Fe<sub>3</sub>O<sub>4</sub>/SnO<sub>2</sub>/graphene composites.

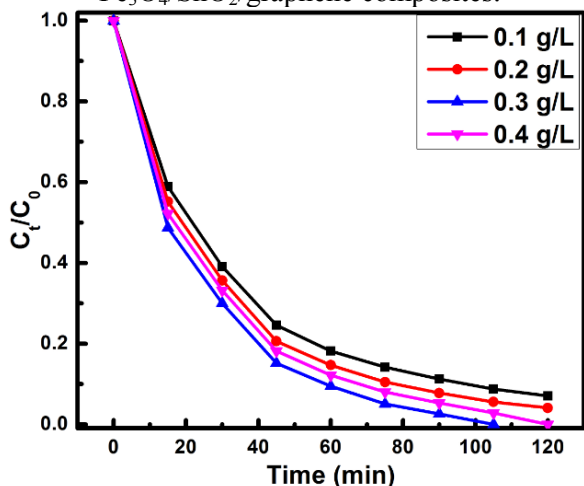


**FIGURE 5.** Effect of dosage on photocatalytic activity of Fe<sub>3</sub>O<sub>4</sub>/SnO<sub>2</sub>/graphene composites.

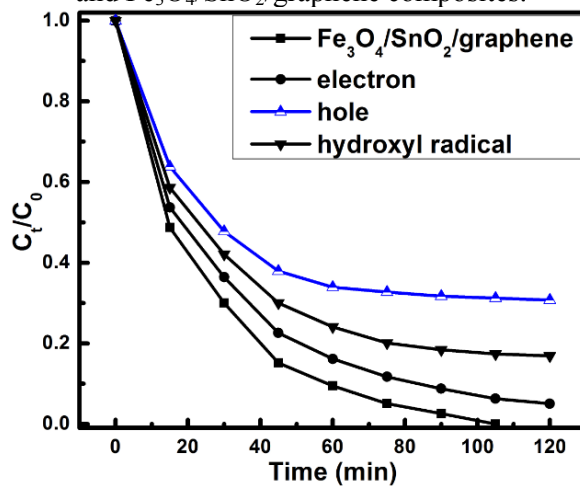


**FIGURE 6.** Effect of scavengers on photocatalytic activity of Fe<sub>3</sub>O<sub>4</sub>/SnO<sub>2</sub>/graphene composites.

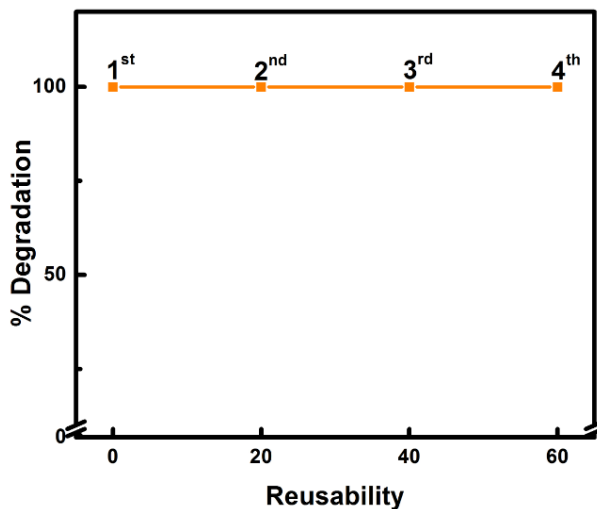


**FIGURE 7.** Reusability of Fe<sub>3</sub>O<sub>4</sub>/SnO<sub>2</sub>/graphene composites.

graphene. The diffraction peaks of SnO<sub>2</sub>, NGP and graphene at Fe<sub>3</sub>O<sub>4</sub>/SnO<sub>2</sub>/NGP and Fe<sub>3</sub>O<sub>4</sub>/SnO<sub>2</sub>/graphene composites are overlapped at 2θ of around 26°. As it is clear from this figure, there is no any impurity in the nanoparticle sample.

The FTIR spectrum of Fe<sub>3</sub>O<sub>4</sub>/SnO<sub>2</sub> nanocomposite, Fe<sub>3</sub>O<sub>4</sub>/SnO<sub>2</sub>/NGP and Fe<sub>3</sub>O<sub>4</sub>/SnO<sub>2</sub>/graphene composites are presented in Fig. 2. Fig. 2f shows the FTIR spectra for Fe<sub>3</sub>O<sub>4</sub>/SnO<sub>2</sub>/NGP composites, while the FTIR spectra for Fe<sub>3</sub>O<sub>4</sub>/SnO<sub>2</sub>/graphene composites is shown in Fig. 2g. The absorption of SnO<sub>2</sub> nanoparticle appears in the range of 540-660 cm<sup>-1</sup> which indicates O-Sn-O and Sn-O stretching vibration modes. The Fe<sub>3</sub>O<sub>4</sub> show the characteristic band of Fe-O stretching vibration at 594 cm<sup>-1</sup> [7]. The absorptions in range of 3400 cm<sup>-1</sup> and 1634 cm<sup>-1</sup> indicate the O-H group stretching and bending vibration modes originating from water molecule [14] while absorption in the range of 1220 cm<sup>-1</sup> and 1527 cm<sup>-1</sup> indicates the C-OH and C-O stretching vibration modes [15,16].

Figure 3 shows the weight loss curve for Fe<sub>3</sub>O<sub>4</sub>/SnO<sub>2</sub>/NGP and Fe<sub>3</sub>O<sub>4</sub>/SnO<sub>2</sub>/graphene composites obtained from TGA measurement. As can be seen, Fe<sub>3</sub>O<sub>4</sub>/SnO<sub>2</sub> nanoparticle do not exhibit the significant percentage loss in the result of TGA measurement. Which indicate that Fe<sub>3</sub>O<sub>4</sub>/SnO<sub>2</sub> nanoparticle without any addition of graphene is stable until 1000°C. The weight loss started around 100°C due to the volatilization of adsorbed water [17]. The weight loss stage from 400°C to 600°C which indicates the combustion effect from NGP and graphene material and thereafter no further decomposition takes place thereafter [18]. Furthermore, the weight loss of graphene at TGA measurement can confirm the existence of the NGP and graphene in Fe<sub>3</sub>O<sub>4</sub>/SnO<sub>2</sub>/NGP and Fe<sub>3</sub>O<sub>4</sub>/SnO<sub>2</sub>/graphene composite samples.

The photocatalytic activities of prepared Fe<sub>3</sub>O<sub>4</sub>/SnO<sub>2</sub>, Fe<sub>3</sub>O<sub>4</sub>/SnO<sub>2</sub>/NGP and Fe<sub>3</sub>O<sub>4</sub>/SnO<sub>2</sub>/graphene catalysts were investigated under UV light irradiation in aqueous solution of methylene blue (MB) dye (Fig 4). It can be seen that photocatalytic activities of Fe<sub>3</sub>O<sub>4</sub>/SnO<sub>2</sub>/graphene composite are obviously better than the Fe<sub>3</sub>O<sub>4</sub>/SnO<sub>2</sub>/NGP composite, especially better than Fe<sub>3</sub>O<sub>4</sub>/SnO<sub>2</sub> nanocomposite. More than 95% of MB has been degraded over them within 90 min. However, only 76.83% and 85.1% of MB could be decomposed over Fe<sub>3</sub>O<sub>4</sub>/SnO<sub>2</sub> and Fe<sub>3</sub>O<sub>4</sub>/SnO<sub>2</sub>/NGP after 120 min, respectively.

Fig. 5 shows the effect of Fe<sub>3</sub>O<sub>4</sub>/SnO<sub>2</sub>/graphene dosage, from 0.1 g/L to 0.4 g/L, on the decolorization efficiency of methylene blue at pH 13. As shown in Fig. 5, maximum degradation at Fe<sub>3</sub>O<sub>4</sub>/SnO<sub>2</sub>/graphene dosages of 0.1 g/L, 0.2 g/L, 0.3 g/L and 0.4 g/L were 92.97%, 95.93% after 120 min, 97.4% after 90 min and 97% after 105 min, respectively. The decreasing maximum degradation at dosage 0.4 g/L it could be due to as the amount of Fe<sub>3</sub>O<sub>4</sub>/SnO<sub>2</sub>/graphene increasing, the scattering of UV by Fe<sub>3</sub>O<sub>4</sub>/SnO<sub>2</sub>/graphene also increased, because of shielding effect [19]. The above observation indicates the optimal Fe<sub>3</sub>O<sub>4</sub>/SnO<sub>2</sub>/graphene dosage was 0.3 g/L.

To know the most involved reactive species MB degradation to the all samples, the addition scavenger was done. In Fig. 6 shows the result of MB degradation in the photocatalytic process with scavenger addition influence. The scavenger addition serves to bind the reactive species to not take role in the photocatalytic process. The result obtained shows that the addition of hole scavenger shows the lowest degradation capacity. This indicates that the most influential reactive species for the samples is hole.

The stability of Fe<sub>3</sub>O<sub>4</sub>/SnO<sub>2</sub>/graphene composite was investigated by a 4-run cycling test under the same condition. For each run, the photocatalyst was recycled, cleaned, and dried from its solutions using magnetic external. The photodegradation efficiency of Fe<sub>3</sub>O<sub>4</sub>/SnO<sub>2</sub>/graphene composite shows no apparent decrease after the 4 reuse cycles, indicating Fe<sub>3</sub>O<sub>4</sub>/SnO<sub>2</sub>/graphene composite is stable (Fig. 7).

#### 4. Conclusion

The hybridizing Fe<sub>3</sub>O<sub>4</sub>/SnO<sub>2</sub> with two different types of graphene material (Fe<sub>3</sub>O<sub>4</sub>/SnO<sub>2</sub>/NGP and Fe<sub>3</sub>O<sub>4</sub>/SnO<sub>2</sub>/graphene) have been successfully synthesized via co-precipitation method. Fe<sub>3</sub>O<sub>4</sub>/SnO<sub>2</sub>/graphene compsite show the best photocatalytic activity under UV light irradiation. More than 95% of MB has been degraded over them within 90 min. The optimum catalyst dosage for Fe<sub>3</sub>O<sub>4</sub>/SnO<sub>2</sub>/graphene composite sample is 0.3 g/L. Scavengers experiment shows that the most

influential reactive species for the samples is hole. Sample showed good cycling capacity result after reuse three times.

## 5. Reference

- [1] Abdessalem Hamrouni, Noomen Moussa, Agatino Di Paola, Leonardo Palmisano, Ammar Houas, Francesco Parrino 2015 *Journal of Photochemistry and Photobiology A: Chemistry* **309** 47-54
- [2] Hadj Benhebal, Messaoud Chaib, Angelique Leonard, Stephanie D. Lambert, Michel Crine 2011 *Journal of Molecular Structure* **1004** 222-226
- [3] Nisha Bayal, P. Jeevanandam 2013 *Materials Research Bulletin* **48** 3790-3799
- [4] Sung Phil Kim, Myong Yong Choi, Hyun Chul Choi 2015 *Applied Surface Science* **357** 302-308
- [5] Huanhao Xiao, Fengyu Qu, Ahmad Umar, Xiang Wu 2016 *Materials Research Bulletin* **74** 284-290
- [6] N. Shanmugam, T. Sathya, G. Viruthagiri, C. Kalyanasundaram, R. Gobi 2016 *Applied Surface Science* **360** 283-290
- [7] Tiejun Xin, Mingliang Ma, Hepeng Zhang, Junwei Gu, Shuangjie Wang, Mengjiao Liu, Qiuyu Zhang 2014 *Applied Surface Science* **288** 51-59
- [8] Zaihua Wang, Yongling Du, Fengyuan Zhang, Zhixiang Zheng, Xiaolong Zhang, Qingliang Feng, Chunming Wang 2013 *Materials Chemistry and Physics* **140** 373-381
- [9] Abdollah Fallah Shojaei, Ali Shams-Nateri, Maryam Ghomashpasand 2015 *Superlattices and Microstructures* **88** 211-224
- [10] Wenjuan Wang, Haipeng Zhang, Ling Zhang, Haiqin Wan, Shourong Zheng, Zhaoyi Xu 2015 *Colloids and Surfaces A: Physicochem. Eng. Aspects* **469** 100-106
- [11] Hui Liu, Tingting Liu, Xiaonan Dong, Yuwu Lv, Zhenfeng Zhu 2014 *Materials Letters* **126** 36-38
- [12] A. Taufik, I. K. Susanto, R. Saleh 2015 *Materials Science Forum* **827** 37-42
- [13] Yue Li, Yanqun Guo, Ruiqin Tan, Ping Cui, Yong Li, Weijie Song 2009 *Materials Letters* **63** 2085-2088
- [14] Qingzhi Luo, Lin Wang, Desong Wang, Rong Yin, Xueyan Li, Jing An, Xiaolian Yang 2015 *Journal of Environmental Chemical Engineering* **3** 622-629
- [15] Lling-Lling Tan, Wee-Jun Ong, Siang-Piao Chai, Abdul Rahman Mohamed 2013 *Nanoscale Research Letters* **8** 465
- [16] Xiaojun Peng, Yang Li, Guoliang Zhang, Fengbao Zhang, Xiaobin Fan, *Journal of Nanomaterials* <http://dx.doi.org/10.1155/2013/841789>
- [17] Lihua Hu, Zhongping Yang, Limei Cui, Yan Li, Huu Hao Ngo, Yaoguang Wang, Qin Wei, Hongmin Ma, Lianguo Yan, Bin Du 2016 *Chemical Engineering Journal* **287** 545-556
- [18] V. Loryuenyong, K. Totepvimarn, P. Eimburanaprat, W. Boonchompoo, A. Buasri 2013 *Advances in Material Science and Engineering* **2013** 923403
- [19] Yu-Ju Chiang, Chia-Chang Lin 2013 *Powder Technology* **246** 137-143